



Kinetic, Equilibrium and thermodynamic studies on the biosorption of Ni(II), Cr(III), and Co(II) from aqueous solutions onto pineapple (*Ananas comosus*) leaf

Adesola Babarinde*, Adeola Ibikunle, Kehinde Awokoya, Segun Ogundare, Adesola Adeleke, Olajumoke Alimi, Yetunde Owosanya, Atinuke Bankole

Department of Chemical Sciences, Olabisi Onabanjo University, Ago-Iwoye, Nigeria

Abstract

The kinetics, equilibrium and thermodynamics of the biosorption of Ni(II), Cr(III), and Co(II) from aqueous solution using the leaf biomass of pineapple (*Ananas comosus*) were investigated under different experimental conditions. Optimum conditions of pH, contact time, biomass dosage, initial metal ion concentration and temperature were determined. The FTIR spectral characteristics of pineapple leaf showed the presence of ionizable groups that could participate in the binding of the metal ions in solution. Kinetic study shows that the pseudo-second-order kinetic model best represents the biosorption of each metal ions. The sorption of each metal ion was analyzed with four isotherm models, in each case, the Freundlich model gave the best isotherm. The study on the effect of dosage shows that the dosage of the biomass significantly affects the uptake of the metal ions from solution.

Thermodynamic parameters such as standard Gibbs-free energy (ΔG°), standard enthalpy (ΔH°), standard entropy (ΔS°), and the activated energy (A) were calculated. The order of spontaneity of the biosorption process was Ni(II)>Co(II)>Cr(III). The activation energy for the biosorption of each of the metal ions was less than 42 kJmol^{-1} at 318K which indicates that each was a diffusion controlled process. The calculated entropy shows that the order of disorderliness is Ni(II) \approx Co(II)>Cr(III).

Key words: pineapple, Ni(II), Co(II), Cr(III), kinetics, isotherm, thermodynamics

Full length article Received: 28-04-2016

Revised: 04-07-2016

Accepted: 15-07-20136

Available online: 31-07-2016

*Corresponding Author, e-mail: adesola.babarinde@oouagoiwoye.edu.ng; Tel:+234-8037232934

1. Introduction

Technological advancement over the years has led to a record level of pollution that now poses a serious threat to man and the environment. The disposal of waste material and heavy metal into the environment is a serious pollution problem affecting water quality. Toxic metals are detrimental to human health. Though, nickel is an essential micronutrient and/or cofactor, it is one of the heavy metal toxicants at higher concentration and is a well-known human carcinogen [1]. The higher concentration of nickel causes dermatitis, nausea, vomiting, behavioral, and respiratory problems in addition to cyanosis, gastrointestinal distress, and weakness [2]. These various processes lead to accumulation of Ni to a toxic

level in the environment, particularly in soil. Human acquire nickel through ingestion of Ni contaminated food, air and water.

All forms of chromium can be toxic at high levels, chromium has been considered as a toxic pollutant and because of its carcinogenic and teratogenic characteristics on the public, it has become a serious health concern [3]. Chromium can be released to the environment through a large number of industrial operations, including tannery industry, metal finishing industry, iron and steel industries and inorganic chemicals production [4]. It is important to remove cobalt from wastewater due to its known toxicity. The effects of acute cobalt poisoning in humans are very serious; among them are asthma-like allergy, damage to

the heart, causing heart failure, damage to the thyroid and liver. Cobalt may also cause mutations (genetic changes) in living cells [5]. Furthermore, metallic cobalt or cobalt sulphate are the most plausible causes of cobalt asthma. Also, cobalt has a role in the development of diffuse interstitial lung disease [6]. With a better awareness of the problems associated with cobalt, research studies related to the method of removing cobalt from wastewater have increasingly drawn attention.

However, agricultural waste beneficiation is a concept that is rapidly gaining interest. Such beneficiation activities include energy production and wastewater treatment. Advanced waste-water treatment methods include ion exchange [7], membrane separation [8], electrolysis [9] and adsorption [10]. Most of these methods are costly, require a high level of expertise and therefore limited in application by several end-users. For these reasons, adsorption technology has gained a wider application due to its inherent low cost, versatility and robustness. Thus, the use of agricultural waste-derived adsorbents for wastewater treatment constitutes the main focus of this study. The main objectives of the present study were to determine the capacity of pineapple leaf for sorption of Ni(II), Cr(III) and Co(II) from solution and to determine the optimum values of the physicochemical parameters which influence the sorption process. The sorption of these metal ions by different biosorbents has been reported but none utilized pineapple leaf, which is an agricultural waste found in different tropical regions of the world.

2. Materials and Methods

2.1. Biomass preparation

Pineapple leaf was obtained from a local market near mini campus of Olabisi Onabanjo University, Ago-Iwoye, Ogun State, Nigeria. The leaves were properly rinsed with water, oven dried at the temperature of about 80°C and cut into pieces of approximately 0.5cm. The leaf sample was kept dried until the time of usage.

2.2. Preparation of solution

All chemicals used in this study were of analytical reagent grade and were used without further purification. Standard solution of each of Ni(II), Cr(III), Co(II) used for this study was prepared from NiCl₂.6H₂O., Cr(NO₃)₃.9H₂O and CoSO₄.7H₂O to make a stock solution of

1000mgL⁻¹ of the metal ion. The working solutions with different concentrations of the Ni(II),Cr(III), Co(II) ions were prepared by appropriate dilutions of the stock solution immediately prior to their use with distilled water. The initial pH of the solution was adjusted accordingly with a pH meter. Each boiling tube used for the biosorption was suspended in a thermostated water bath. The concentration before and after biosorption of each metal ion was determined using a Perkin-Elmer analyst 700 Flame Atomic Absorption Spectrophotometer (FAAS) with deuterium background corrector. Fourier Transform Infrared (FTIR) spectra of dried unloaded biomass and metal loaded biomass were recorded at 400-4000cm⁻¹, using a Shimadzu FTIR model 8400 S spectrophotometer.

2.3. FT-IR analysis

The functional groups present on the surface of pineapple leaf would give insight to the biosorption capacity of the biomass. These groups would form active sites for sorption on the material surface. Therefore, the FT-IR spectra of dried unloaded and metal-loaded pineapple leaves were taken to obtain information on the nature of possible interactions between the functional groups of pineapple leaf and each of Ni(II), Cr(III), and Co(II) in solution.

2.4. Batch biosorption study

In order to explore the effects of pH, contact time, biosorbent dose, initial metal ion concentration and temperature, a series of batch studies were conducted at 27°C using thermostated water bath. The biosorption study was carried out by contacting 0.5g of the pineapple leaf with 25ml of the metal ion solution under different conditions for a period of time in a boiling tube. The residual metal ion was analyzed using atomic absorption spectrophotometer. The amount of metal ion biosorbed from solution was determined by difference.

2.5. Effect of pH on biosorption

The effect of pH on the biosorption of Ni(II),Cr(III), Co(II) ions was carried out within 1 ≤ pH < 7 to prevent the precipitation of the metal ions. This was done by contacting 0.5g of pineapple (*Ananas comosus*) leaf with 25ml of 100 mgL⁻¹ each of Ni(II), Cr(III), and Co(II) solution in glass tubes. The pH of each solution was adjusted to the desired value by drop wise addition of 0.1M HNO₃ and/or 0.1M NaOH. The

glass tubes containing the mixture were suspended in a water bath for three hours. The biomass was removed from the solution by decantation. The residual metal ion concentration in the solution was analyzed. The optimum pH was determined as the pH with the highest biosorption of Ni(II), Cr(III), Co(II).

2.6. Effect of contact time on biosorption

The biosorption of the metal ions by pineapple leaf was studied at various time intervals (0 to 360 min) and at a concentration of 100 mgL⁻¹. This was done by weighing 0.5 g of pineapple leaf into each boiling tube and 25 ml of 100 mgL⁻¹ of metal ion solution at optimal pH was introduced into it. The leaf was left in the solution for varying periods of time. The solution in the boiling tube was decanted and analysed using an FAAS. The amount of metal ions biosorbed was calculated for each sample.

2.7. Effect of biomass dosage on biosorption

In this study, different biosorbent dosages were selected ranging from 0.2 - 2.0 g while concentration of each metal ion was fixed at 100 mgL⁻¹. The effect of sorbent dose on the uptake of the metal ion was carried out by contacting different masses of pineapple leaf with 25 ml of 100 mgL⁻¹ solution of the metal ion for at optimal pH and time.

2.8. Effect of initial concentration on biosorption

Batch biosorption study of metal ion was carried out using a concentration range of 10 to 100 mgL⁻¹. This was done by introducing 0.5 g of the pineapple leaf into each of the boiling tubes employed and 25 ml solution at optimal pH was added to the tube. Two boiling tubes were used for each concentration. The tubes were left in a thermostated water bath maintained at 27°C. The pineapple leaf was removed from the solution and the concentration of residual metal ion in each solution was determined.

2.9. Effect of temperature on biosorption

The batch biosorption process was studied at different temperatures of 20 to 50°C in order to investigate the effect of temperature on the biosorption process. This was done by contacting 0.5 g of pineapple leaf with 25 ml of 100 mgL⁻¹ of metal ion solution at the optimal pH. The biosorption of metal ion may involve chemical bond formation and ion exchange since the temperature is a main parameter affecting them

2.10. Statistical analyses

The curve fittings of the data obtained were performed using Microcal Origin 6.0 software.

3. Results and discussion

3.1. FT-IR studies of the free and metal-bound pineapple Leaf

The FT-IR spectra of dried unloaded, Ni-loaded, Cr-loaded and Co-loaded pineapple (*A. Comosus*) leaf were taken to obtain information on the nature of possible interactions between the functional groups of pineapple leaf biomass and the metal ions as presented in Figure 1. The IR spectra pattern of the biomass showed distinct and sharp absorptions indicative of the existence of the -OH and C=O groups as shown in Figure 1. These bands are due to the functional groups of pineapple (*A. Comosus*) leaf that participate in the biosorption of Ni(II), Cr(III) and Co(II). On comparison, there are clear band shifts and decrease in intensity of bands as reported in Table 1. The FT-IR spectra of the pineapple (*A. Comosus*) leaf biomass indicated slight changes in the absorption peak frequencies due to the fact that the binding of the metal ions causes reduction in absorption frequencies. This shift in absorbance observed implies that there were metal binding processes taking place on the active sites of the biomass. Analysis of the FT-IR spectra showed the presence of ionizable functional groups (C=O, O-H) which are able to interact with cations [11 – 14]. This implies that these functional groups would serve in the removal of positively charged ions from solution.

3.2. Effect of solution pH on metal ion biosorption

The pH of solution has been established to be a vital parameter in biosorption process [13, 15, 16]. The net charge of the sorbate and that of the sorbent are dependent on the pH of the solution. At low pH, the metal ion uptake is inhibited by net positive charge on the sorbent and the competition between the metal ions and the hydrogen ions in solution. As the pH increases, the negative charge density on biomass increases as a result of deprotonation of the metal binding sites on the leaf, consequently, the biosorption of the metal ions increases.

Figure 2 shows the variation of the metal ion biosorbed on pineapple (*A. comosus*) leaf at various solution pH values. In each case, the biosorption increased steadily as the pH increased from pH 1 to pH 6. The increase observed in the

biosorption with increase in pH implies that ion-exchange process is involved. The reaction involved the biosorption of metal ion (represented as M^{X+} for a metal ion) from the liquid phase to the solid phase, the biosorbent with lone pair of electrons (represented as \ddot{A}), and can be considered as a reversible reaction with an equilibrium being made between the two phases as schematically shown below for a divalent metal ion in solution:



The reversibility of the biosorption process is observed when the metal-bound biomass is treated with dilute HNO_3 which is a desorption process.

3.3. Biosorption kinetics

The dependence of the biosorption of each metal ion at its optimal pH is presented in Figure 3. It was observed that the sorption of each metal ion by pineapple (*A. comosus*) leaf was highly influenced by contact time. The data obtained from the sorption of metal ions onto pineapple leaves showed that the biosorption increased with increasing contact time. The biphasic plot shows an initial rapid stage (fast phase) where biosorption is fast and contributes to equilibrium uptake and a second stage (slow phase) whose contribution to the metal ion biosorption is relatively smaller. The fast phase is the instantaneous biosorption stage, it is assumed to be caused by external biosorption of metal ion to the leaf surface. The second phase is a gradual biosorption stage, which is diffusion rate controlled. Finally, the biosorption sites are used up, the uptake of the metal ion reached equilibrium. This phase mechanism has been suggested to involve two diffusion processes, external and internal, respectively [17]. The biosorption of each of the three metal ions achieves equilibrium within 3 hr although their rates of uptake are different. This might be due to the differences in hydrated ionic sizes of the metal ions [18]. Different kinetic models are needed to establish the mechanism of a biosorption process [19]. In order to investigate the kinetics of the biosorption of these metal ions on pineapple (*A. comosus*) leaf, four kinetic models were employed. These are the pseudo-first-order, the pseudo-second-order, Elovich and the Intraparticle equations.

One of such models is the Lagergren pseudo-first-order model which considers that the rate of

occupation of the biosorption sites is proportional to the number of the unoccupied sites [14]:

$$rate = -\frac{d[A]}{dt} = k [A]^n \quad (2)$$

Which can also be written as

$$\frac{d}{dt} q_t = k_1 (q_e - q_t) \quad (3)$$

Integrating between the limits $q_t = 0$ at $t = 0$ and $q_t = q_t$ at $t = t$, we obtain

$$\log \left[\frac{q_e}{(q_e - q_t)} \right] = \frac{k_1}{2.303} t \quad (4)$$

This can be rearranged to obtain a linear form:

$$\log(q_e - q_t) = \log q_e - \frac{k_1}{2.303} t \quad (5)$$

Where k_1 is the Lagergren rate constant of the biosorption (min^{-1}); q_e and q_t are the amounts of metal ions sorbed (mg g^{-1}) at equilibrium and at time t , respectively. The plot of $\log(q_e - q_t)$ versus t for the biosorption of metal ions on the biomass at initial concentration of 100 mgL^{-1} should give a straight line for a process that follows first-order kinetic model as shown in Figure 4. The data was equally subjected to the pseudo-second-order kinetic model. The pseudo-second-order kinetic model is represented as

$$\frac{d}{dt} q_t = k_2 (q_e - q_t)^2 \quad (6)$$

On integrating between boundary conditions, we have

$$\frac{1}{q_e - q_t} = \frac{1}{q_e} + k_2 t \quad (7)$$

On rearrangement, we have

$$\frac{t}{q_t} = \frac{1}{k_2 q_e^2} + \frac{1}{q_e} t \quad (8)$$

Where k_2 is the equilibrium rate constant of pseudo-second-order biosorption process ($\text{g mg}^{-1} \text{min}^{-1}$). In the three metal ions under study, the straight line plots of t versus t/q_t showed good fitness of experimental data with the second-order kinetic model for different initial concentrations of the three metal ions as presented in Figure 5. The data were equally subjected to the Elovich kinetic model given by

$$q_t = A + B \ln t \quad (9)$$

The intraparticle diffusion equation given as

$$R = K_s t^b \quad (10)$$

Has been used to indicate the behaviour of intraparticle diffusion as the rate limiting step in the biosorption process. R is the percent metal biosorbed, K_s is the intraparticle diffusion constant; t is the contact time, while b is the gradient of the linear plot. In the linear form, equation (10) turns to

$$\log R = b \log t + \log K_s \quad (11)$$

Out of the four kinetic models tested, the correlation coefficients were found to be highest for the pseudo-second-order kinetic equation and in each case it is in excess of 0.99 as presented in Table 2. Pseudo-second-order kinetic model is the best kinetic model to predict the dynamic biosorption of Ni(II), Cr(III) and Co(II) on pineapple (*A. comosus*) leaf. The result shows that the rate of biosorption of the metal ions is of the order Co(II) > Ni(II) > Cr(III) which may be due to the differences in hydrated ionic sizes of the ions in solution [18]. The biosorption capacity is in the order Ni(II) ≈ Co(II) > Cr(III). This implies that the amount of each metal biosorbed depends on its valency.

3.4. Biosorption isotherms

The adsorption isotherm studies were carried out at different concentration from 10 to 100 mg L⁻¹ the isotherm data obtained were analyzed with four isotherm models.

The Langmuir isotherm was used to describe observed sorption phenomena and suggests that uptake occurs on a homogenous surface by monolayer sorption without interaction between adsorbed molecules. The linear form of the Langmuir equation is expressed as

$$\frac{1}{q_e} = \frac{1}{q_{\max} K_L} \frac{1}{C_e} + \frac{1}{q_{\max}} \quad (12)$$

Where C_e is the equilibrium concentration of metal ion (mg L⁻¹), q_e is the amount of metal ion biosorbed per specific amount of biosorbent (mg g⁻¹), q_{\max} is the maximum biosorption capacity (mg g⁻¹), and K_L is equilibrium constant (L mg⁻¹) related to energy of biosorption which quantitatively reflects the affinity between the biosorbent and the biosorbate. Where q_{\max} and K_L can be determined from the linear plot of $1/q_e$ versus $1/C_e$. The shape of the Langmuir isotherm can be used to predict whether a sorption is favourable or unfavourable in a batch biosorption process. The essential features of the isotherm can

be expressed in terms of a dimensionless constant separation factor, R_L , which is defined [20] as

$$R_L = \frac{1}{1 + K_L C_i} \quad (13)$$

Where C_i is the initial concentration (mg L⁻¹) and K_L is the Langmuir equilibrium constant (L mg⁻¹). The value of the separation factor, R_L , provides vital information about the nature of biosorption. The value of R_L implies the type of Langmuir isotherm to be reversible ($R_L=0$), favourable ($0 < R_L < 1$), linear ($R_L=1$), or unfavourable ($R_L > 1$) The Langmuir isotherm is presented in Figure 9 while the evaluated constants are given in Table 3. The Freundlich Isotherm is an empirical equation describing adsorption onto a heterogenous surface. The Freundlich isotherm is expressed as

$$\log \Gamma = \frac{1}{n} \log C_e + \log K_f \quad (14)$$

Where K_f and n are the Freundlich constants related to the biosorption capacity (mg g⁻¹) and biosorption intensity of the biosorbent, respectively. Figure 10 illustrates the biosorption isotherm of the metal ions pineapple leaf. The isothermal parameters are presented in Table 3. The Temkin Isotherm model was also used to fit the experimental data. Unlike the Langmuir and Freundlich, the Temkin isotherm takes into account the interactions between biosorbents and metal ions to be biosorbed and it is based on the assumption that the free energy of sorption is a function of the surface coverage [21]. The linear form of the Temkin isotherm is represented as:

$$q = B \ln A + B \ln C_e \quad (15)$$

Where C_e is concentration of the biosorbate at equilibrium (mg L⁻¹), q_e is the amount of adsorbate adsorbed at equilibrium (mg g⁻¹). $RT/b_T = B$ where T is the temperature (K) and R is the ideal gas constant (8.314 J mol⁻¹ K⁻¹) and A and b_T are constants. A plot of q_e versus $\ln C_e$ enables the determination of constants A and b_T . The constant B is related to the heat of adsorption and A is the equilibrium binding constant (L min⁻¹) corresponding to the maximum binding energy. The Dubinin-Radushkevich (D-R) isotherm model was used to estimate the heterogeneity of the surface energies. The D-R isotherm equation is linearly represented as

$$\ln q = \ln q_m - \beta \varepsilon^2 \quad (16)$$

$$\varepsilon = RT \ln \left(1 + \frac{1}{C_e} \right) \quad (17)$$

where q_m is the theoretical saturation capacity (mol g^{-1}), β is a constant related to the mean free energy of adsorption per mole of the adsorbate ($\text{mol}^2\text{J}^{-2}$), and ϵ is the polanyi potential, C_e is the equilibrium concentration of adsorbate in solution (mol/L), R ($\text{J mol}^{-1}\text{K}^{-1}$) is the gas constant and T (K) is the absolute temperature. The D-R constants q_m and β were calculated from the linear plots of $\ln q_e$ versus ϵ^2 of Figure 12 are presented in Table 3. The constant β gives an idea about the mean free energy E (J mol^{-1}) of biosorption per molecule of the biosorbate when it is transferred to the surface of the solid from infinity in the solution and can be calculated from the relationship [22]

$$E = \frac{1}{\sqrt{2\beta}} \quad (18)$$

If the magnitude of E is between 8 and 16 kJ mol^{-1} , the sorption process is supposed to proceed via chemisorption but if E is less than 8 kJ mol^{-1} , the sorption process is of physical nature [22].

3.6. Biosorption thermodynamics

The variation of temperature affects the biosorption of metal ions onto solid surfaces of biomass since the biosorption process is a reversible one. The nature of each side of the equilibrium determines the effect temperature has on the position of equilibrium. The side that is endothermic is favoured by increase in temperature while the contrary holds for the exothermic side. The corresponding free energy change was calculated from the relation [13, 23].

$$\Delta G^0 = -RT \ln K_c \quad (19)$$

Where T (K) is the absolute temperature. The equilibrium constant (K_c) was calculated from the following relationship:

$$K_c = \frac{C_{ad}}{C_e} \quad (20)$$

Where C_e and C_{ad} are the equilibrium concentrations of metal ions (mg L^{-1}) in solution

and on biosorbent, respectively. Consequently, the thermodynamic behavior of the biosorption of

Ni(II), Cr(III) and Co(II) onto pineapple leaf was evaluated through the change in free energy (ΔG^0), enthalpy (ΔH^0) and entropy (ΔS^0). The thermodynamic parameters like enthalpy and entropy are obtained using van't Hoff equation [24]. The change in free energy is related to other thermodynamic properties as:

$$\Delta G^0 = \Delta H^0 - T\Delta S^0 \quad (21)$$

$$\ln K_c = \frac{\Delta S^0}{R} - \frac{\Delta H^0}{RT} \quad (22)$$

Where T is the absolute temperature (K); R is the gas constant ($8.314 \text{ J mol}^{-1}\text{K}^{-1}$). ΔH^0 (J mol^{-1}) and ΔS^0 ($\text{J mol}^{-1}\text{K}^{-1}$) were calculated from the slope and intercept of the linear plot of $\ln K_c$ vs $1/T$. The thermodynamic parameters obtained for this study are presented in Table 4. The plots shown in Figure 14 are linear over the entire range of temperature investigated.

The negative values of ΔG^0 indicate spontaneity of each biosorption process, with the order of spontaneity being $\text{Ni(II)} > \text{Co(II)} > \text{Cr(III)}$. The positive values of ΔH^0 for the biosorption of the three metal ions suggest endothermic nature of the biosorption processes. This is also supported by the increase in the value of biosorption capacity of the biosorbent with rise in temperature. The positive value of ΔH^0 indicates the presence of an energy barrier in the biosorption process. Similarly, the ΔS^0 values are positive indicating increase in randomness during the biosorption process for these three metal ions. These positive values of ΔS^0 observed for the biosorption of these metal ions indicates an increase in randomness at the solid/solution interface during their biosorption. The order of disorderliness being $\text{Ni(II)} > \text{Co(II)} > \text{Cr(III)}$.

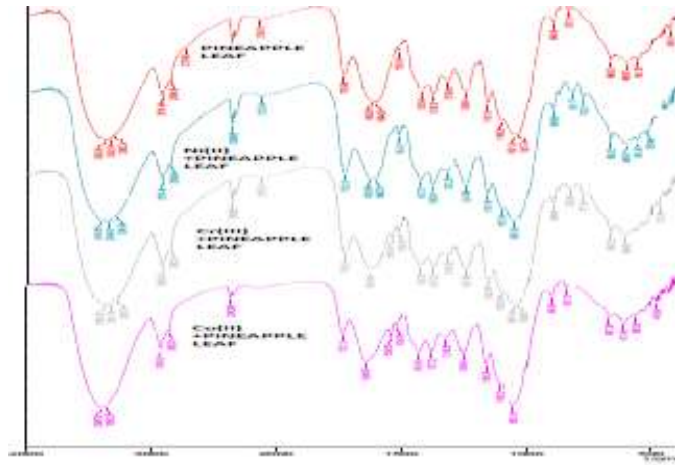


Figure 1: FT-IR Spectra for free and Ni(II), Cr(III), and Co(II) bound pineapple leaf

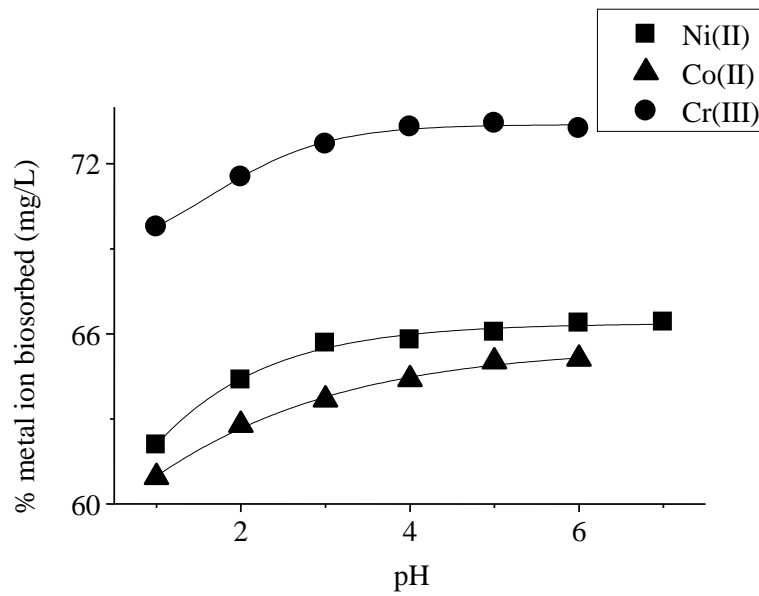


Figure 2: pH dependent profile of the biosorption of Ni(II), Cr(III) and Co(II) by pineapple (*A. Comosus*) leaf

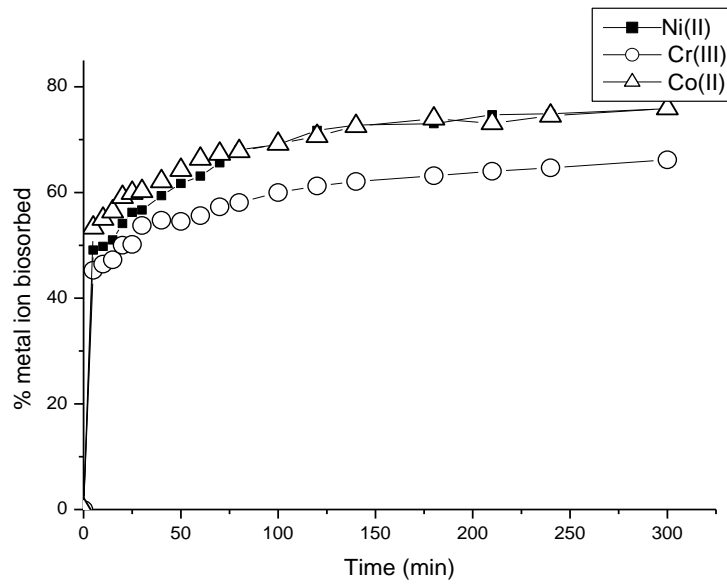


Figure 3: Time dependent profile of the biosorption of Ni(II), Cr(III) and Co(II) by pineapple (*A. Comosus*) leaf

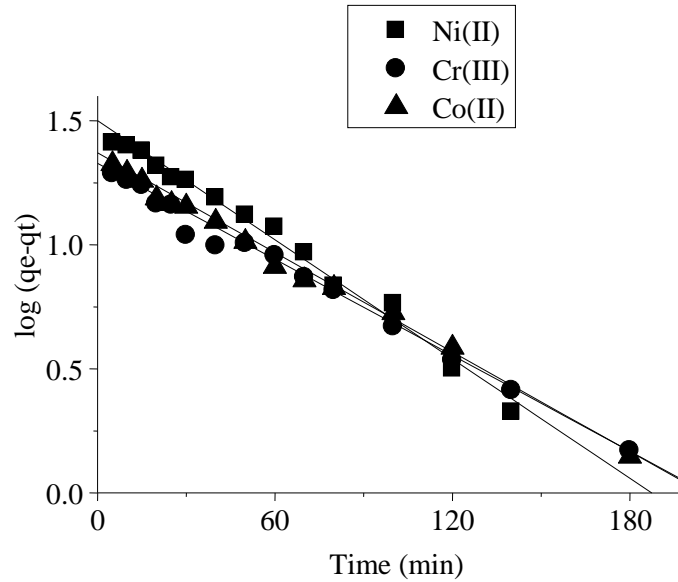


Figure 4: The pseudo-first-order plot for the biosorption of Ni(II), Cr(III) and Co(II) by pineapple (*A. Comosus*) leaf

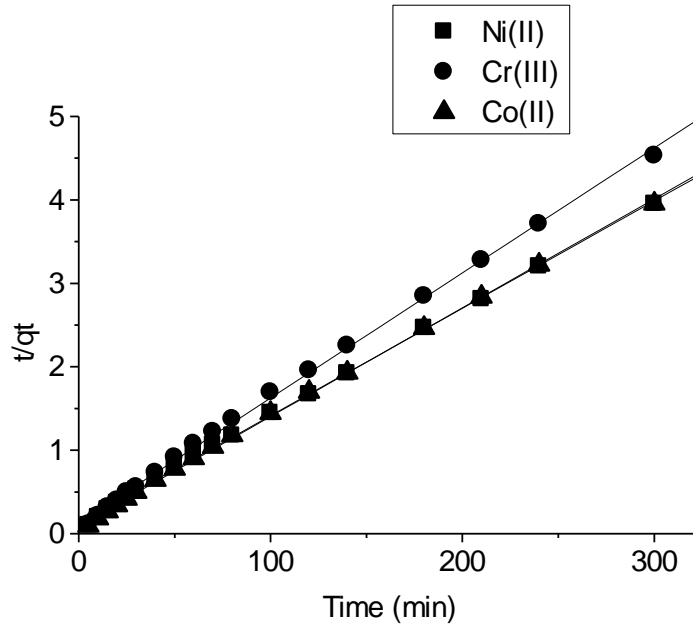


Figure 5: The pseudo-second-order plot for the biosorption of Ni(II), Cr(III) and Co(II) by pineapple (*A. Comosus*) leaf

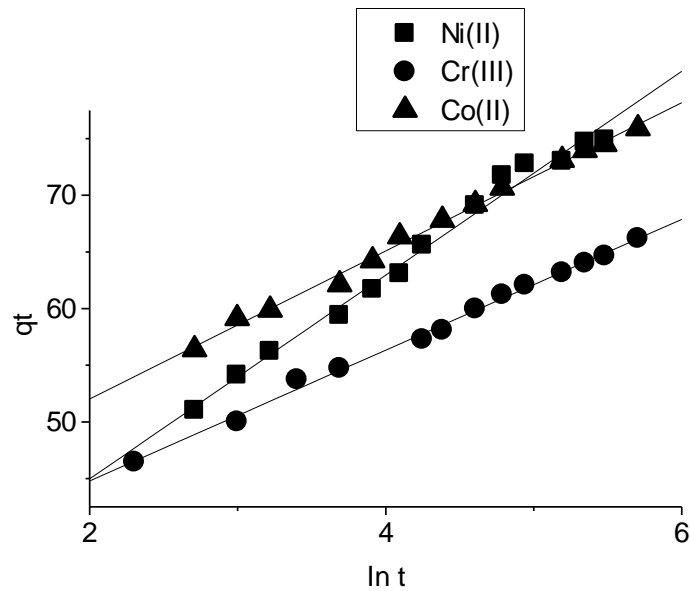


Figure 6: Elovich plot for the biosorption of Ni(II), Cr(III) and Co(II) by pineapple (*A. Comosus*) leaf

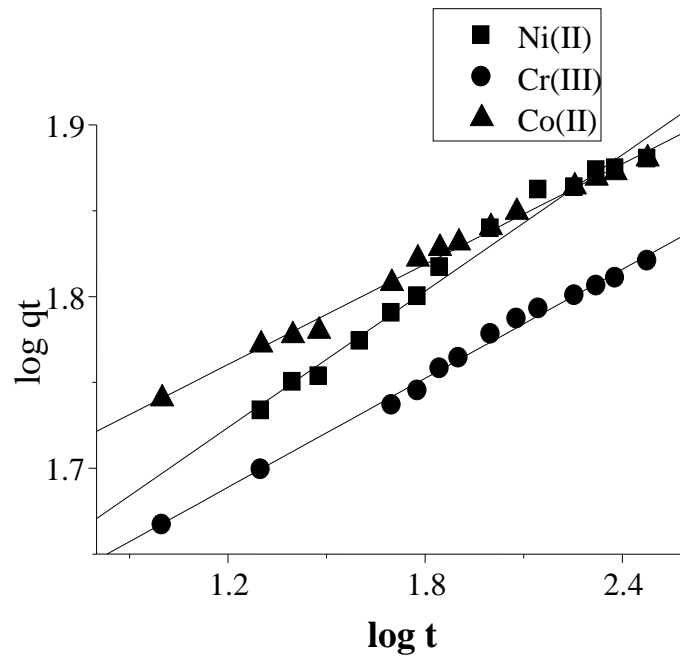


Figure 7: Intraparticle graph for the biosorption of Ni(II), Cr(III) and Co(II) by pineapple leaf

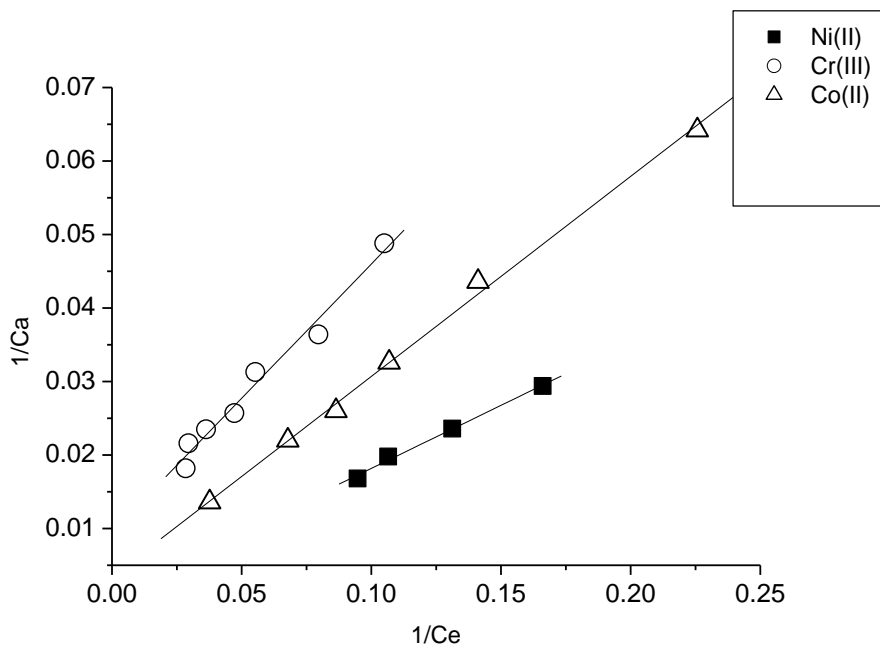


Figure 9: Langmuir Isotherm for biosorption of Ni(II), Cr(III) and Co(II) by pineapple leaf

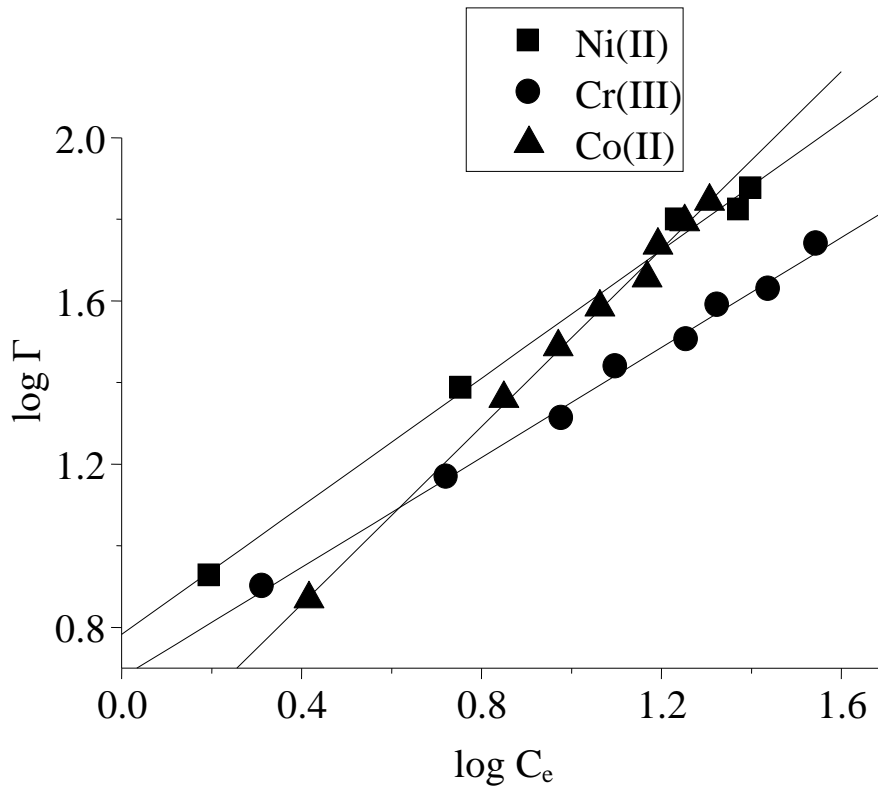


Figure 10: Freundlich Isotherm for biosorption of Ni(II), Cr(III) and Co(II) by pineapple leaf

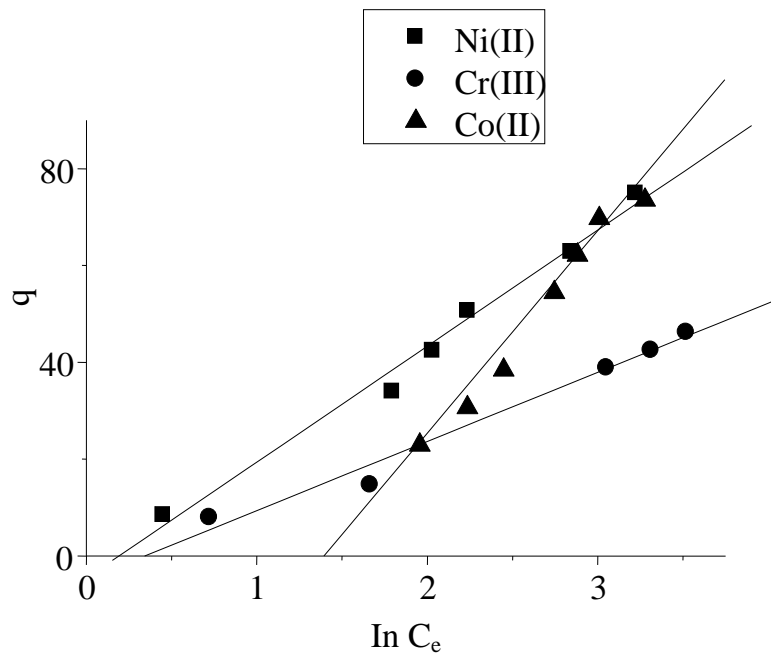


Figure 11: Temkin isotherm for the biosorption of Ni(II), Cr(III), Co(II) using pineapple Leaf

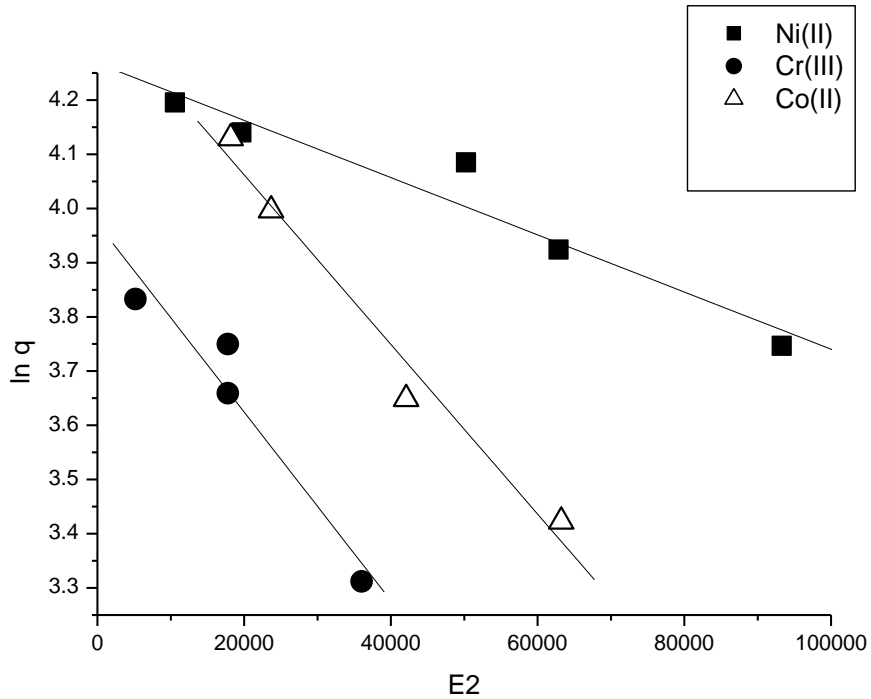


Figure.12: Dubinin-Radushkevich isotherm for the biosorption of Ni(II), Cr(III), Co(II) using pineapple leaf

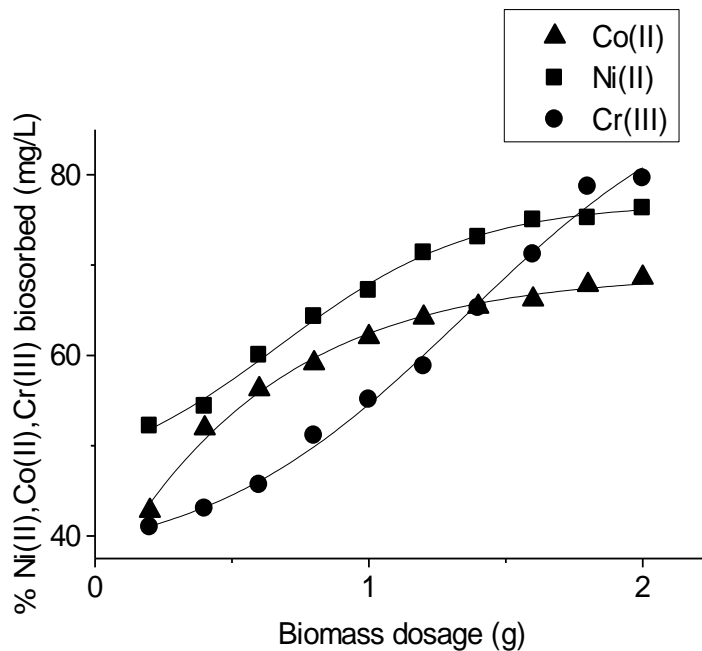


Figure 13: Effect of biosorbent dose on the biosorption of Ni(II), Cr(III) and Co(II) by pineapple (*A. Comosus*) leaf at 100 mgL^{-1} initial metal ion concentration.

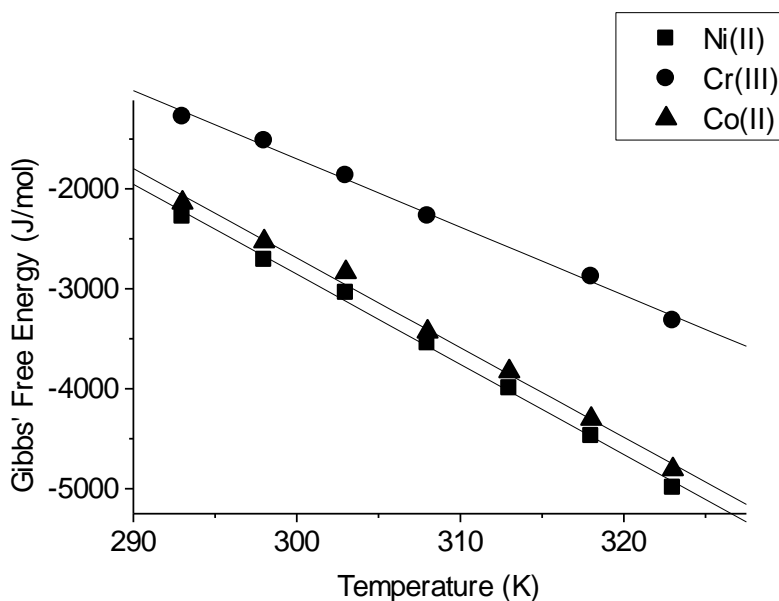


Figure 14: Free energy change for the biosorption of Ni(II), Cr(III) and Co(II) onto pineapple leaf

Table 1: FT-IR Spectra Characteristics of pineapple (*A. Comosus*) leaf before and after biosorption of Ni(II), Cr(III) and Co(II) for 2 h

Metal ion	Absorption band (cm^{-1})			Functional group
	Before	After	Difference	
Ni(II)	3383.26	3416.05	+32.79	O-H Stretch
Cr(III)	3383.26	3383.26	0	O-H Stretch
Co(II)	3383.26	3396.76	+13.5	O-H Stretch
Ni(II)	1249.91	1247.99	-1.92	C-O Stretch (Carboxylic acid)
Cr(III)	1249.91	1247.99	-1.92	C-O Stretch (carboxylic acid)
Co(II)	1249.91	1249.91	0	C-O Stretch (Carboxylic acid)
Ni(II)	1161.19	1161.19	0	C-O Stretch (Alcohol)
Cr(III)	1161.19	1159.26	-1.93	C-O Stretch (Alcohol)
Co(II)	1161.19	1159.26	-1.93	C-O Stretch (Alcohol)
Ni(II)	1735.99	1732.19	-3.8	C=O Stretch
Cr(III)	1735.99	1732.13	-3.86	C=O Stretch
Co(II)	1735.99	1732.13	-3.86	C=O Stretch

Table 2: Kinetic parameters for the biosorption of Ni(II), Cr(III) and Co(II) onto pineapple leaf at 100 mgL⁻¹

Kinetic model	Parameters	Ni(II)	Cr(III)	Co(II)
Pseudo-first-order	q _e (mgg ⁻¹)	31.2	20.2	22.1
	k ₁ (min ⁻¹)	1.838x10 ⁻²	1.458 x 10 ⁻²	1.508 x 10 ⁻²
	R ²	0.9887	0.9917	0.9953
Pseudo-second-order	q _e , cal(mgg ⁻¹)	77.7	66.8	76.7
	k ₂ (g mg ⁻¹ min ⁻¹)	1.3054 x 10 ⁻³	1.741 x 10 ⁻³	1.707 x10 ⁻³
	R ²	0.999	0.9986	0.9991
Elovich	A	26.9846	33.2522	38.9358
	B	8.9931	5.7705	6.5404
	R ²	0.9885	0.9958	0.9953
Intraparticle diffusion	K _d (mgg ⁻¹ min ^{-1/2})	36.3640	35.3574	43.5331
	B	0.1063	0.1423	0.0991
	R ²	0.9946	0.9915	0.9947

Table 3: Isothermal parameters for the biosorption of Ni(II), Cr(III) and Co(II) onto pineapple leaf at 100 mgL⁻¹

Isotherm	Parameters	Ni(II)	Cr(III)	Co(II)
Freundlich	n	1.2742	1.489	0.9179
	K _F (mgg ⁻¹)(Lmg ¹) ^{1/n}	6.0633	4.7967	2.6398
	R ²	0.9941	0.9949	0.9970
Langmuir	q _{max} (mgg ⁻¹)	1000	105.596	289.01
	K _L (L mg ⁻¹)	5.82x10 ⁻³	2.5938x10 ⁻²	1.2709x10 ⁻²
	R ²	0.9972	0.9891	0.9987
Temkin	A	-4.7369	-5.012	-62.1321
	B(mgg ⁻¹)	23.9607	14.27	42.3998
	R ²	0.9935	0.9899	0.9888
D-R	q _m (mgg ⁻¹)	71.3637	53.1055	79.4454
	β(mol ² J ⁻²)	5.2677 x 10 ⁻⁶	1.7394 x 10 ⁻⁵	1.5646 x 10 ⁻⁵
	E(Jmol ⁻¹)	435.7019	239.773	252.81
	R ²	0.9357	0.9291	0.9759

Table 4: Thermodynamic parameters for the biosorption of Ni(II), Cr(III) and Co(II) onto pineapple (*A. Comosus*) leaf

	$\Delta H^{\circ}(kJmol^{-1})$	$\Delta S^{\circ}(Jmol^{-1})$	R^2	SD	$A(kJmol^{-1})@303K$	$A(kJmol^{-1})@318K$
Ni(II)	+24.1829	+90.1	0.9969	59.50982	26.70	26.82
Cr(III)	+18.7698	+68.2	0.9963	54.17588	21.28	21.41
Co(II)	+24.1942	+89.6	0.9955	71.59615	26.71	26.83

3.5. Effect of dosage on biosorption

The effect of biomass dosage on biosorption efficiency is reported in Figure 13. The general trend of increase in metal ion biosorbed with increase in biomass dosage indicates an increase in uptake due to more binding sites on the biomass available for biosorption. Such trend has been reported for other biosorbents.

4. Conclusion

Biosorption of Ni(II), Cr(III), and Co(II) by *A. comosus* leaf biomass is found to be influenced by the solution pH, contact time, initial metal ion concentration, biosorbent dose, and temperature. The pH has much effect on the biosorption of these metal ions from aqueous solutions. The kinetic studies indicate that the biosorption process follows pseudo-second-order kinetics. Equilibrium studies show that the biosorption of Ni(II), Cr(III), Co(II) ions are well represented by Freundlich gave best fit out of the four models tested. The thermodynamic study shows that the biosorption of each of Ni(II), Cr(III) and Co(II) was spontaneous. This study shows that pineapple leaf has high potential for treating industrial effluents containing Ni(II), Cr(III) and Co(II).

REFERENCES

[1] M.G. Maleva., G.F. Nekrasova., P. Malec., M. N.V. Prasad and K. Strzalka. (2009). Ecophysiological tolerance of *Elodea Canadensis* to nickel exposure. *Chemosphere*.77 (3) 392-398.
 [2] N. Akhtar., J. Iqbal. and M. Iqbal. (2004). Removal and recovery of nickel(II) from aqueous solution by loofa sponge-immobilized biomass of *Chlorella sorokiniana*: characterization studies. *Journal of Hazardous Materials*. 108 (1-2). 85-94
 [3] O.D. Uluozlu., O.D. Sari and M. Tuzen. (2010). Biosorption of antimony from aqueous

solution by lichen (*Physcia tribacia*). *Chemical Engineering Journal* 163: 382 -388.

[4] H. Gao., Y. Liu., G. Zeng., W. Xu., T. Li and W. Xia. (2007). Characterization of Cr IV removal from aqueous solutions by a surplus agricultural waste Rice straw. *Journal of Hazardous Materials*. 150(2): 446-452.

[5] S. Rangaraj and S.H. Moon. (2002). Kinetics of adsorption of Co(II) removal from water and wastewater by ion exchange resins. *Water Res*. 36: 1783-1793.

[6] A. Linna., P. Oska., P. Palmroos., P. Roto., P. Laippala and J. Uitti. (2003). Respiratory health of cobalt Production workers. *Am. J. Ind. Med*. 44: 124-132.

[7] S.A. Cavaco., S. Fernandes., M.M. Quina and L.M. Ferreira. (2007). Removal of chromium from electroplating industry effluents by ion exchange resins. *Journal of Hazardous Materials* 144: 634-638

[8] V. Mavrov., S. Stamenov., E. Todorova., H. Chmiel and T. Erwe. (2006). Removal of nickel ions from wastewater by Mg(OH)₂/MgO nanostructures embedded in Al₂O₃ membranes. *J. Alloys Compd*. 426: 281-285.

[9] K. Kurt., O. Apaydin and M.T. Gonullu. (2007). Reduction of COD in wastewater from an organized Tannery industrial region by Electro-Fenton process. *Journal of Hazardous Materials*. 143: 33-40.

[10] M.S. Onyango., Y. Kojima., O. Aoyi., E.C. Bernardo and M.H. Hitoki. (2004). Adsorption equilibrium modeling and solution chemistry dependence of fluoride removal from water by trivalent-cation-exchanged zeolite F-9. *J. Colloid Interface Sci*. 279: 341-350.

[11] S. Pradhan., S. Singh and L.C. Rain. 2007. Characterization of various functional groups

present in the capsule of *Microcystis* and study of their role in biosorption of Fe, Ni and Cr. *Bioresource Technology* 98: 595-601.

[13] X. F. Sun., S.G. Wang., X.W. Liu., W.X. Gong., N. Bao., B.Y. Gao., and H.Y. Zhang. (2008). Biosorption of Malachite Green from Aqueous Solutions onto Aerobic Granules: Kinetic and Equilibrium Studies. *Bioresource Technology*. 99: 3475 – 3483.

[12] B.Y.O. Bueno., M.L.Torem., F. Molina and L.M.S. de Mesquita. (2008). Biosorption of Pb(II), Cr(III) and Cu(II) by *R. opacus*: equilibrium and kinetic studies. *Minerals Engineering*. 21(1): 6575.

[14] N. Ertugay and Y.K. Bayhan. (2008). Biosorption of Cr(VI) from aqueous solutions by biomass of *Agaricus bisporus*. *Journal of Hazardous Materials*. 154: 432- 439.

[15] N.A.A. Babarinde, J.O. Babalola, A.O. Ogunfowokan, A.C. Onabanjo. (2009). Kinetic, equilibrium, and thermodynamic studies of the biosorption of cadmium (II) from solution by *Stereophyllum radiculosum*. *Toxicological & Environmental Chemistry*. 91(5) 911 – 922.

[16] N.A.A. Babarinde., J.O. Babalola., J. Adegoke., A.O. Osundeko., S. Olasehinde., A. Omodehin and E. Nurhe. (2012). Biosorption of Ni(II), Cr(III), and Co(II) from solutions using *Acalypha hispida* Leaf: Kinetics, Equilibrium, and Thermodynamics. *Journal of Chemistry* vol 2013, Article ID 460635: 1-8.

[17] Y. Wu., L. Zhang., C. Gao., X. Ma and R. Han. (2010). Adsorption of copper ions and methylene Blue in a Single and Binary System on Wheat straw. *Journal of Chemical Engineering Data*. 54: 3229-3234.

[18] J. Kielland. (1937). Effective diameters of unhydrated and hydrated ions. *Journal of American Chemical Society*. 59 1675-1678.

[19] A. Y. Okasha and H.G. Ibrahim. 2010. Removal of Cu²⁺ ions from aqueous solutions by adsorption on Libyan soil. *J. Environ. Sci. Eng.* 4 (10): (35) 9 -15

[20] T.S. Anirudhan and P.G. Radhakrishnan. (2008). Thermodynamics and kinetics of adsorption of Cu(II) from aqueous solutions onto a new cation exchanger derived from tamarind fruit shell. *Journal Chemical Thermodynamics*. 4(4):702- 709.

[21] Z. Chen., W. Ma and M. Han. (2008). Biosorption of nickel and copper onto treated alga (*Undaria pinnatifida*): Application of isotherm and kinetic models. *Journal of Hazardous Materials*, 155(1-2):327-333..

[22] S. Kundu and A.K. Gupta. (2006). Arsenic adsorption onto iron oxide-coated cement (IOCC): regression analysis of equilibrium data with several isotherm models and their optimization. *Chemical Engineering Journal*. 122 (1-2):93-106.

[23] G. de la Rosa., H.E. Reynel-Avila., A. Bonilla-Petriciolet., I. Cano-Rodríguez., C. Velasco-Santos., R. Martínez-Elangovan., L. Pilip and K. Chandraraj. (2008). Biosorption of Chromium Species by Aquatic Weeds: Kinetics and Mechanism Studies. *Journal of Hazardous Materials*. 152:100-12.

[24] R.Y. Qu., C. Zhang., C. Sun., C. Wang., C. Ji., H. Chen and P. Yin. (2010). Adsorption of Hg(II) from an Aqueous Solution by Silica-Gel Supported Diethylenetriamine Prepared via Different Routes: Kinetics, Thermodynamics and Isotherms. *Journal of Chemical Engineering Data*. 55:1496–1504.